

## Local Movement in the S2 Region of the Voltage-Gated Potassium Channel hKv2.1 Studied Using Cysteine Mutagenesis

C. J. Milligan and D. Wray

School of Biomedical Sciences, University of Leeds, Leeds LS2 9JT, England

**ABSTRACT** The positively charged S4 region of voltage-dependent potassium channels moves outward during depolarization, leading to channel opening, but possible movement of the negatively charged S2 region may be more complex. Here we have studied possible movement of the S2 region of the slowly activating human voltage-dependent potassium channel hKv2.1. For this, cysteine mutants in the S2 region were expressed in *Xenopus* oocytes by injection of cRNA. Whole-cell currents were measured using the two-electrode voltage-clamp technique, and the effect of the membrane-impermeable cysteine-binding reagent parachloromercuribenzenesulfonate (PCMBS) was studied. For mutant S223C (located just outside the membrane in the S2 region), PCMBS inhibited currents and caused faster deactivation of tail currents. The time course of reactivity of PCMBS on tail current amplitudes was faster at more negative holding potentials. There was no effect of PCMBS on potassium channel currents for mutants D225C, N226C, A230C, and V232C. These data suggest that residue S223 is exposed to the extracellular phase at normal resting potentials, making it accessible to PCMBS, but upon depolarization there is a conformational change, making it less accessible, possibly by a local rather than global movement of S2 residues into the membrane. Voltage-dependent movements of nearby residues could also explain the results.

### INTRODUCTION

Voltage-gated potassium channels play an important role in controlling electrical activity and proper functioning of excitable cells. Numerous voltage-gated outward-rectifying potassium channels have now been cloned and share a common structure comprising four  $\alpha$ -subunits surrounding a central aqueous pore, with each  $\alpha$ -subunit consisting of six hydrophobic transmembrane segments, S1–S6 (reviewed by Armstrong and Hille, 1998; Pongs, 1992). The human hKv2.1 (DHK1 or hDRK1) channel belongs to this family of voltage-gated outward rectifier potassium channels and is characterized by slowly activating currents, noninactivating currents when expressed in *Xenopus* oocytes (Albrecht et al., 1993).

The roles played by some of the transmembrane domains have been extensively studied. The S4 segment consists of conserved basic residues at every third position, and detailed work has shown that this segment plays an important role in voltage sensing by the channel (Liman et al., 1991; Papazian et al., 1991; Logothetis et al., 1992; Perozo et al., 1993; Shao and Papazian, 1993; Aggarwal and MacKinnon, 1996). The S2 and S3 segments contain negatively charged residues, and more recent work has also begun to implicate these regions in voltage sensing (Papazian et al., 1995; Planells-Cases et al., 1995; Seoh et al., 1996; Tiwari-Woodruff et al., 1997). The linker between the S5–S6 segments (H5 or P region) contains a highly conserved sequence that is invaginated into the membrane from the extracellular face

and lines the outer mouth of the pore, forming the selectivity filter (MacKinnon and Yellen, 1990; Hartmann et al., 1991; Yellen et al., 1991; Yool and Schwartz, 1991; Doyle et al., 1998). The S5 and S6 regions line the part of the pore internal to the selectivity filter (Choi et al., 1993; Kirsch et al., 1993; Lopez et al., 1994; Holmgren et al., 1997).

More recently, studies of conformational changes in channels have been made using cysteine-scanning mutagenesis. More specifically, movement of the S4 region during depolarization has been demonstrated by the application to *Shaker* potassium channels of membrane-impermeable cysteine-binding reagents (Larsson et al., 1996; Yusaf et al., 1996; Baker et al., 1998), thus probing the accessibility of cysteine-mutated residues. In this way it was possible to show that, upon depolarization, the S4 segment appears to move outward by around seven amino acids. Complementary to this approach has been the use of fluorescent cysteine-binding probes, which provide useful information on changes in the local environment of S4 during depolarization (Mannuzzu et al., 1996). Strong electrostatic interactions exist between the negatively charged residues in S2/S3 and the positive residues in S4; these interactions are important for folding and functioning of the channel (Papazian et al., 1995; Tiwari-Woodruff et al., 1997). It seems plausible to hypothesize that as the S4 transmembrane segment moves outward upon depolarization, the S2 segment, with its negatively charged residues, might move inward. Studies have been made of the changes in the local environment of the S2 region of the *Shaker* channel, using fluorescent probes (Cha and Bezanilla, 1997), and local rather than global movements of the S2 region have been suggested.

To investigate possible movement of the S2 region in this paper, we have used cysteine-binding reagents to study the accessibility of residues in the S2 region under varying degrees of depolarization. For this we have used cysteine

Received for publication 11 February 1999 and in final form 13 December 1999.

Address reprint requests to Prof. D. Wray, Biomedical Sciences, University of Leeds, Leeds LS2 9JT, England. Tel.: 44-113-233-4320; E-mail: d.wray@leeds.ac.uk.

© 2000 by the Biophysical Society

0006-3495/00/04/0110 \$2.00

mutants of the human K<sup>+</sup> channel clone hKv2.1, and we have tested accessibility using the membrane-impermeable sulfhydryl-reactive reagent parachloromercuribenzenesulfonate (PCMBs) in voltage-clamped oocytes. This reagent has already proved useful in inhibiting currents in the S4 region (Yusaf et al., 1996).

## MATERIALS AND METHODS

### Preparation of DNA

The hKv2.1 clone in pGEM-He-Juel (provided by O. Pongs, Hamburg, Germany) was transformed into *Escherichia coli* DH5 $\alpha$  competent cells (Sambrook et al., 1989). DNA was isolated with a miniprep kit (Promega) according to the manufacturer's instructions.

### Preparation of mutants

The mutants S223C, D225C, N226C, Q228C, A230C, and V232C were produced by polymerase chain reaction (PCR) methods (Innis et al., 1990). PCR reactions were carried out (Sambrook et al., 1989) using Pfu polymerase enzyme for 30 cycles (40 s at 95°C, 1 min at 60–66°C, and 2 min at 72°C).

First-round PCR reactions were carried out using a forward primer, 5'-ATGCCGGCGGGCATGACGAA-3', and a reverse mutagenic primer (incorporating the desired base change), as well as a forward mutagenic primer and a reverse primer, 5'-ACAATTTTCCCAGGAGAGTCTTG-3'. Second-round PCR extension was carried out using the above products and the above forward and reverse primers, to produce a ~1-kb product. This latter product was then digested with the restriction enzymes *Ppu*MI and *Apa*I to produce a 250-bp fragment. The wild-type hKv2.1/pGEM-He-Juel was also digested with the same enzymes, and the mutagenic 250-bp fragment was ligated using T<sub>4</sub> ligase. The induced mutations were verified by dideoxy sequencing (Sambrook et al., 1989).

To make RNA, the cDNAs for hKv2.1 were linearized with *Nor*I, and capped cRNA was transcribed using T7 polymerase via a MEGAscript kit (Ambion). The RNA concentration was estimated using a Tris-acetate EDTA agarose gel and comparing with standard markers.

### Electrophysiology

*Xenopus* oocytes (Dumont stage V or VI) were prepared and injected with cRNA, and electrophysiological recordings were made as previously described (Wilson et al., 1994). Briefly, oocytes were injected with 50 nl (containing 0.1–2.0 ng cRNA) of wild-type or mutant cRNA. Oocytes were then incubated, at 19.7°C, for 24–48 h, in multiwell tissue culture plates (one oocyte per well) containing modified Barth's solution (88 mM NaCl, 1 mM KCl, 2.4 mM NaHCO<sub>3</sub>, 0.82 mM MgSO<sub>4</sub>, 0.33 mM Ca(NO<sub>3</sub>)<sub>2</sub>, 0.4 mM CaCl<sub>2</sub>, 7.5 mM Tris-HCl, pH 7.6, 10,000 U/L penicillin, 100 mg/L streptomycin). To record expressed membrane currents from oocytes, the oocytes were held in a recording chamber (50  $\mu$ l volume) and continually perfused (2 ml/min) at room temperature (normally 22–25°C) with Ringer's solution (115 mM NaCl, 2 mM KCl, 1.8 mM CaCl<sub>2</sub>, 10 mM HEPES, adjusted to pH 7.2 with NaOH). Membrane currents were recorded by the two-electrode voltage-clamp technique with a Geneclamp 500 amplifier (Axon Instruments). The amplifier was controlled via a CED 1401 Plus interface and CED software. The current signal was sampled at 4 kHz and filtered at 2 kHz. Electrodes were filled with 3 M KCl (0.5–2.0 M $\Omega$  resistance). To construct current-voltage relationships, the membrane potential was held at –80 mV, and 500-ms duration test depolarizations (at 0.1 Hz) were applied in 10-mV increments, from –70 mV to +70 mV, and peak current amplitudes were measured. Twenty 10-mV hyperpolarizing

steps (500 ms, 0.5 Hz) were applied and used to remove leak and capacitance currents. PCMBs was applied by continuous perfusion during repetitive step depolarizations (500 ms, 0.1 Hz, +40 mV) from the selected holding potential (usually –80 mV). To study tail currents, oocytes were perfused with high potassium solution (100 mM KCl, 2 mM MgCl<sub>2</sub>, 1.0 mM CaCl<sub>2</sub>, 10 mM HEPES, pH 7.2), and test pulses were applied at 0.1 Hz. The membrane potential was held at the selected holding potential (usually –80 mV), and 100 ms prepulses to +40 mV were applied, followed by 350-ms test pulses in 10-mV increments from 0 mV to –110 mV. Tail-current amplitudes were measured 2 ms after the end of the prepulse, and the deactivation time course was fitted to a single exponential. Exponential fits to the deactivation time course were also used to determine tail-current amplitudes by extrapolation back to the end of the prepulse (particularly where PCMBs affected the time course); this method gave results similar to those obtained by measurement of the current amplitude at 2 ms (as expected, because deactivation time constants were much longer than this), so the latter method was generally used. PCMBs was applied at different holding potentials during repetitive stimulation, the time constant of reactivity of PCMBs was obtained by fitting current amplitudes to a single-exponential curve for each cell, and mean values were obtained.

Many of the results for the mutants tested gave no effect of PCMBs, and the data for these are described but generally are not shown in this paper, in the interest of brevity and clarity. Data are expressed as the mean  $\pm$  standard error of the mean (SEM), and Student's *t*-test was used to test statistical significance.

## RESULTS

### Characterization of wild-type and mutant currents

The membrane topology of hKv2.1 is illustrated in Fig. 1, which also shows the residues that have been mutated into cysteines in the S2 domain and in the S1/S2 linker. The wild-type or mutant cRNA was injected into *Xenopus* oocytes, and voltage-clamp recordings were made after 24–48 h.

Characteristics of the wild-type channel are shown in Fig. 2. Mean current-voltage (*I*-*V*) curves, shown in Fig. 2 *A*, were obtained during step depolarizations from –80 mV, and the voltage dependence expected for this outwardly-rectifying channel can be seen (Albrecht et al., 1993). Fig. 2 *B* shows example recordings and illustrates the slow activation time course and the minor inactivation characteristic of the hKv2.1 channel. Wild-type tail currents were recorded in high potassium solution (see Materials and Methods) during steps after a +40-mV, 100-ms prepulse; an example recording is shown in Fig. 2 *D*. The mean tail-current *I*-*V* curve is shown in Fig. 2 *C*, reversing at around –5 mV as expected; mean deactivation time constants are plotted against voltage in Fig. 2 *E*.

All the mutants studied produced functional channels when expressed in oocytes, except for Q228C, which did not display detectable currents. The *I*-*V* curves for the mutants S223C (Fig. 4 *B*), D225C, N226C, A230C, and V232C (data not shown) were similar to the wild-type *I*-*V* curves. The time courses (typical examples shown in Fig. 3) of the mutant currents were generally similar to wild type with slow activation and little inactivation, except for



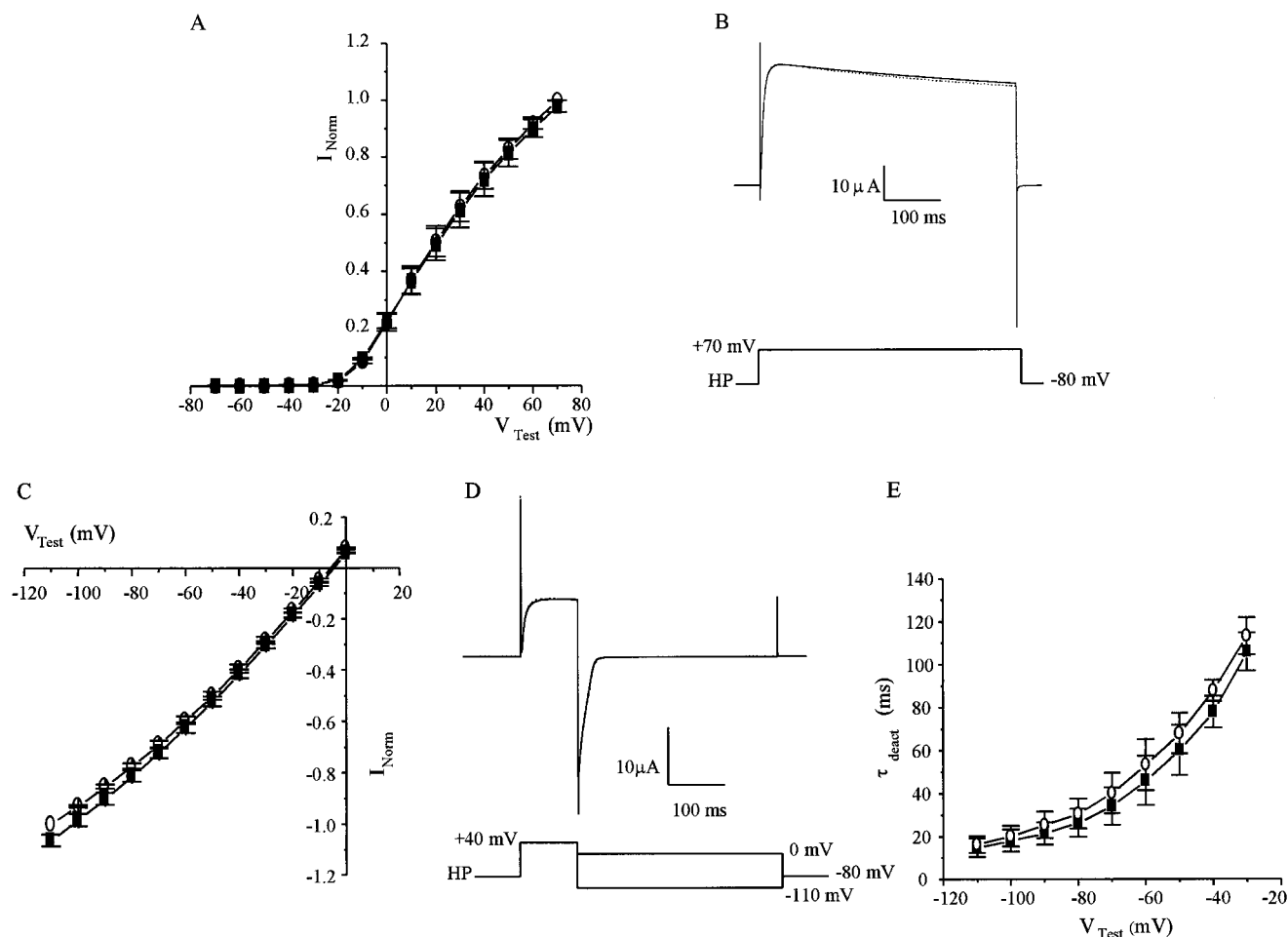


FIGURE 2 Characterization of hKv2.1 wild-type currents expressed in *Xenopus* oocytes. (A) Wild-type current-voltage relationship curves before ( $\circ$ ) and after ( $\blacksquare$ ) the application of PCMBS (100  $\mu$ M), using the repetitive stimulation protocol (see Materials and Methods). Currents were normalized with respect to the control current amplitude obtained in the absence of PCMBS at a test potential of +70 mV (control current amplitude  $12.3 \pm 0.1 \mu\text{A}$ ,  $n = 4$ ). (B) Current traces recorded for steps from -80 mV to +70 mV before (—) and after (---) application of PCMBS (100  $\mu$ M). (C) Tail current-voltage relationship curves in high potassium solution (100 mM) before ( $\circ$ ) and after ( $\blacksquare$ ) application of (100  $\mu$ M) PCMBS. The reagent was applied for 2 min at a holding potential of -80 mV in the absence of stimulation followed by washing. For the construction of tail current  $I$ - $V$  curves, oocytes were held at -80 mV and subjected to 100-ms prepulses to +40 mV followed by 350-ms test pulses (every 10 s) to evoke tail currents. Tail currents were normalized with respect to the control amplitude recorded at -110 mV in the absence of PCMBS (control amplitude  $-26.3 \pm 1.7 \mu\text{A}$ ,  $n = 5$ ). (D) Tail current traces recorded at -110 mV before (—) and after (---) application of (100  $\mu$ M) PCMBS. (E) Deactivation time constants ( $\tau_{\text{deact}}$ ) before ( $\circ$ ) and after ( $\blacksquare$ ) application of PCMBS (100  $\mu$ M) ( $n = 5$ ). These were obtained by exponential fits to the tail currents using the same experimental data as in Fig. 2 C. In all graphs in the figure, the mean  $\pm$  SEM is shown, and there were no significant differences between the values in the presence and absence of PCMBS for the graphs shown in A, C, and E.

tivation time constants and for the time course of reactivity of PCMBS on tail-current amplitude. Channel opening per se was not required for PCMBS action, while reversal of the effect by DTT confirmed a specific action via binding to cysteine at 223.

### Effects of other cysteine-binding reagents

The effects of PCMBS described above were not large, so we have investigated whether other cysteine-binding reagents (methanethiosulfonate ethyltrimethylammonium, MTSET, and thimerosal) had a greater effect and so might

be easier to characterize. As for PCMBS, these reagents had no effect on wild-type currents (Fig. 6, A and C). For mutant S223C, MTSET produced an inhibition of  $\sim 12\%$  ( $p < 0.05$ ), and this was also reflected in the inhibition of the  $I$ - $V$  curve in a voltage-independent way (Fig. 6 B). For thimerosal applied to this mutant, there was a small increase in currents (by  $\sim 10\%$ ,  $p < 0.05$ ) with a corresponding small increase in the  $I$ - $V$  curve, again voltage-independent (Fig. 6 D).

Thus the other cysteine-binding reagents tested (MTSET and thimerosal) had no greater effect than PCMBS and were therefore not examined further. MTSET produced an inhib-

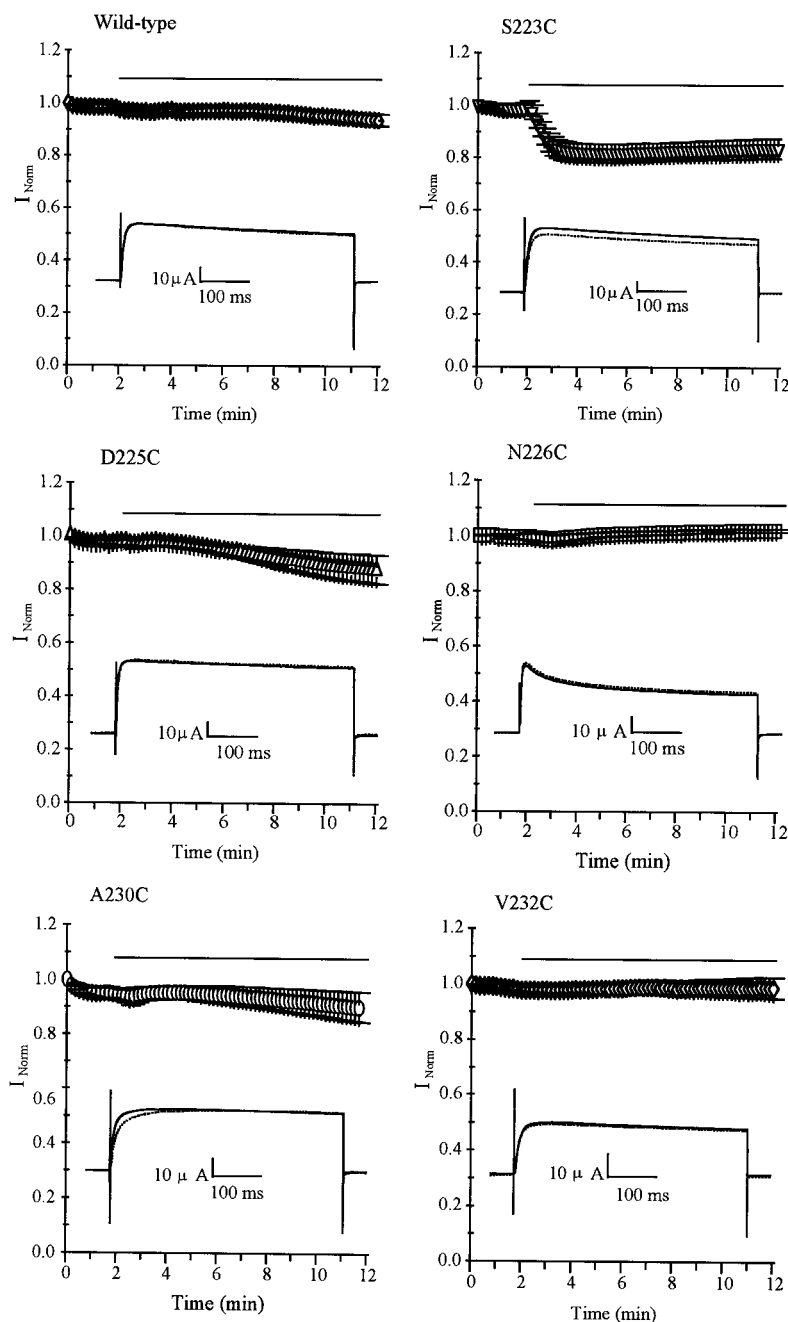


FIGURE 3 Effect of PCMBs on potassium currents for wild-type and mutant channels S223C, D225C, N226C, A230C, and V232C. Oocytes were perfused with PCMBs (100  $\mu$ M) over the time indicated by the solid bars, and oocytes were repetitively depolarized by stepping from a holding potential of  $-80$  mV to  $+40$  mV for 500 ms every 10 s. Current amplitudes have been normalized with respect to the value recorded over the first 2 min of the experiment. Initial values of current were  $19.7 \pm 3.9$   $\mu$ A,  $n = 8$  (wt),  $27.9 \pm 3.8$   $\mu$ A,  $n = 11$  (S223C),  $11.7 \pm 2.7$   $\mu$ A,  $n = 5$  (D225C),  $29.0 \pm 3.4$   $\mu$ A,  $n = 4$  (N226C),  $9.7 \pm 1.3$   $\mu$ A,  $n = 4$  (A230C) and  $28.0 \pm 1.8$   $\mu$ A,  $n = 5$  (V232C). Insets show typical current traces recorded during the construction of  $I$ - $V$  curves before (—) and after (····) the application of PCMBs, and are for a test potential of  $+70$  mV. Mean  $\pm$  SEM values from 4–11 oocytes for each mutant are shown. The S223C current amplitude was significantly reduced by PCMBs ( $p < 0.05$ ) for  $t > 2.5$  min as compared to wild-type and to initial current values. PCMBs had no significant effect on the current amplitude of the other mutants when compared to wild type.

itory affect, as has generally been observed elsewhere (Larsson et al., 1996), while thimerosal produced a small increase, as has also been seen for other channels (Yao et al., 1997).

## DISCUSSION

In the experiments reported here, mutants S223C, D225C, N226C, Q228C, A230C, and V232C of the human outward-rectifier hKv2.1 were studied. Mutant Q228C did not express detectable currents in oocytes, while the other mutants

displayed  $I$ - $V$  curves similar to those of wild-type channels, although some of the mutants displayed altered time courses. Mutation to cysteine of some of the residues produced kinetic changes; the time courses of inactivation and deactivation were altered for mutants N226C and D225C, respectively. These residues may have roles in channel function.

The membrane-impermeable cysteine-binding reagent PCMBs was without effect on wild-type and mutant currents, except for mutant S223C, where there was a partial inhibition of currents. Furthermore, other cysteine-binding



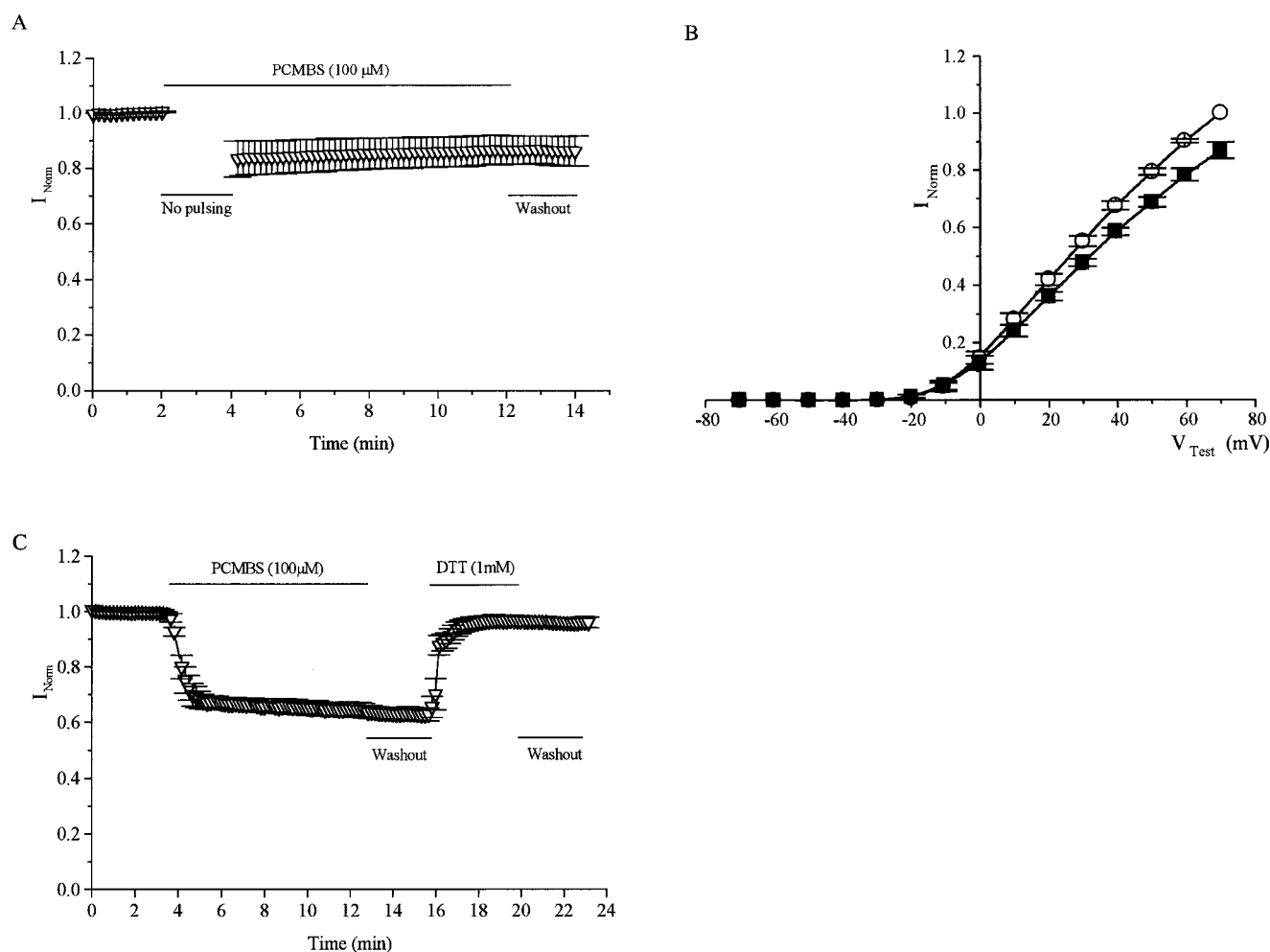


FIGURE 4 Effect of PCMBs on potassium currents for mutant S223C. (A) Oocytes were repetitively stimulated by stepping from a holding potential of  $-80$  mV to  $+40$  mV for 500 ms every 10 s. Stimulation was stopped for a period of 2 min, during which PCMBs ( $100 \mu\text{M}$ ) was applied (solid bar) and then stimulation restarted. Current amplitudes were normalized to the value recorded over the first 2 min of the experiment. The initial current value was  $16.3 \pm 4.2 \mu\text{A}$ ,  $n = 6$ . (B) Current-voltage relationship curves before (○) and after (■) the application of PCMBs ( $100 \mu\text{M}$ ) from the same experiments as above. Currents were normalized to the value in the absence of PCMBs at a test potential of  $+70$  mV ( $I_{\text{Norm}}$ ) (current amplitude  $15.1 \pm 2.8 \mu\text{A}$ ,  $n = 6$ ). (C) Reversal of inhibition of S223C mutant currents by PCMBs with dithiothreitol (DTT). Oocytes were perfused with PCMBs ( $100 \mu\text{M}$ ), washed, and then DTT ( $1 \text{ mM}$ ) (as shown by the bars) was applied. Current amplitudes were normalized to the value recorded over the first 2 min of the experiment. The initial current value was  $23.9 \pm 2.1 \mu\text{A}$ . Values shown are the mean  $\pm$  SEM.

reagents tested (MTSET and thimerosal) had effects on mutant S223C but not on wild type. These results, together with the reversal of the effect of PCMBs by DTT, show that the cysteine at residue 223 specifically binds these reagents and that this residue is accessible and hence exposed from the extracellular side.

There were voltage-dependent effects of PCMBs when it was applied to mutant S223C, which were studied in detail for tail currents and are summarized in Fig. 5. The time course of reactivity of PCMBs on tail current amplitudes was faster at more negative potentials. These voltage-dependent results for the S223C mutant suggest that this residue is more accessible to the extracellular phase at hyperpolarized potentials. At very negative potentials, the

deactivation time constant was less affected by PCMBs, but possibly this could be the result of a secondary effect rather than a decrease in accessibility, because the best measure of accessibility is the time of reactivity with PCMBs.

The decrease in accessibility at depolarized potentials can be explained by an expected movement of the negatively charged S2 region into the membrane when the cell is depolarized. A possible scenario for this could be local movement of residue S223 rather than movement as a whole of the S2 region. However, changes in accessibility could also come about, for instance, by some local occluding conformational change of adjacent regions/residues of the protein, so exposing or occluding S223 during potential changes. So for instance, the effect could arise as a side

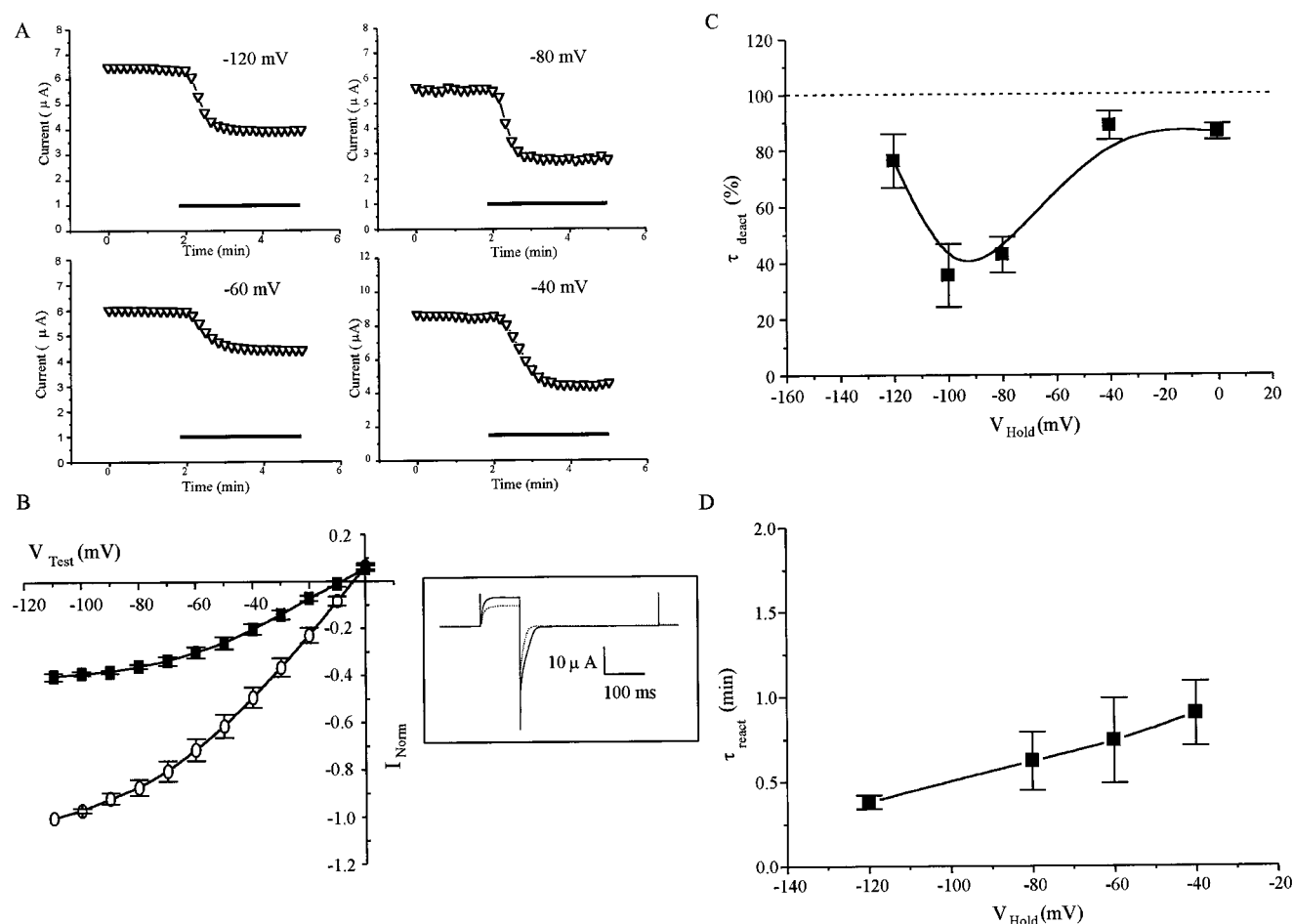


FIGURE 5 Voltage-dependent effects of PCMBs on mutant S223C channel currents. (A) Mutant S223C tail currents were produced by repetitive stimulation at 0.1 Hz. Oocytes (maintained in high potassium solution, 100 mM) were perfused with PCMBs (100  $\mu$ M) as shown by the bars, and tail-current amplitudes were measured at -100 mV (100 ms) after 100-ms prepulses to +40 mV from holding potentials of -120, -80, -60, and -40 mV. Current amplitudes for S223C were significantly reduced by PCMBs ( $p < 0.05$ ) at all holding potentials as compared to initial current amplitude. (B) Effect of PCMBs on tail-current  $I$ - $V$  curves for the S223C mutant channel. The  $I$ - $V$  curves were obtained before (○) and after (■) the application of PCMBs (100  $\mu$ M) in the same experiments as in (A) for a holding potential of -80 mV throughout. Tail currents were normalized to the current value in the absence of PCMBs ( $I_{Norm}$ ) (current amplitude  $-4.8 \pm 1.1$   $\mu$ A,  $n = 3$ ). Values shown are the mean  $\pm$  SEM. Current amplitudes were significantly reduced by PCMBs when compared to the currents in the absence of PCMBs ( $p < 0.05$ ) at test potentials of  $\leq -20$  mV (paired  $t$ -tests). The inset shows a typical recording before (—) and after (····) the application of PCMBs at a holding potential of -80 mV for a tail-current test potential of -110 mV. (C) Deactivation time constants ( $\tau_{deact}$ ) are plotted against the holding potential at which PCMBs (100  $\mu$ M) was applied. Deactivation time constants were measured for tail currents, using a holding potential of -80 mV and a test potential of -60 mV. Stimulation was then stopped, and PCMBs (100  $\mu$ M) was then applied for 2 min at different holding potentials ( $V_{hold}$ ), followed by washing for 2 min and then by a further measurement of deactivation time constant from a holding potential of -80 mV. Data are plotted as a percentage of the initial value of the time constant before the application of PCMBs. (D) The time constant of reactivity ( $\tau_{react}$ ) of PCMBs is plotted against the holding potential at which PCMBs was applied. The data are from experiments as in (A) above ( $n = 3$ –5).

effect of possible movement of the S3-S4 linker, as in the helical screw model (Durell and Guy, 1992). However, such proposed movement of the S3-S4 linker may in fact not occur, and it could remain fairly stationary (Aggarwal and MacKinnon, 1996; Mathur et al., 1997).

Our results showing a lack of effect of PCMBs on the other residues suggest either that amino acids D225, N226, A230, and V232 are not accessible to PCMBs or that binding of the reagent does not affect function. A reasonable suggestion is that residues 230 and 232 are not exposed to

the extracellular environment, consonant with the proposed intramembrane (i.e., inaccessible) location of these residues. For residues 225 and 226, either they are not critical for function (indicating a *local* effect of PCMBs on residue 223), or they are not accessible to PCMBs (possibly because residues 225 and 226 are closer to the membrane than 223, and so might be obstructed by neighboring structures).

The effects of PCMBs on mutant S223C were small compared with the much larger effects seen in studies of the S4 region with this reagent (Yusaf et al., 1996). This partial

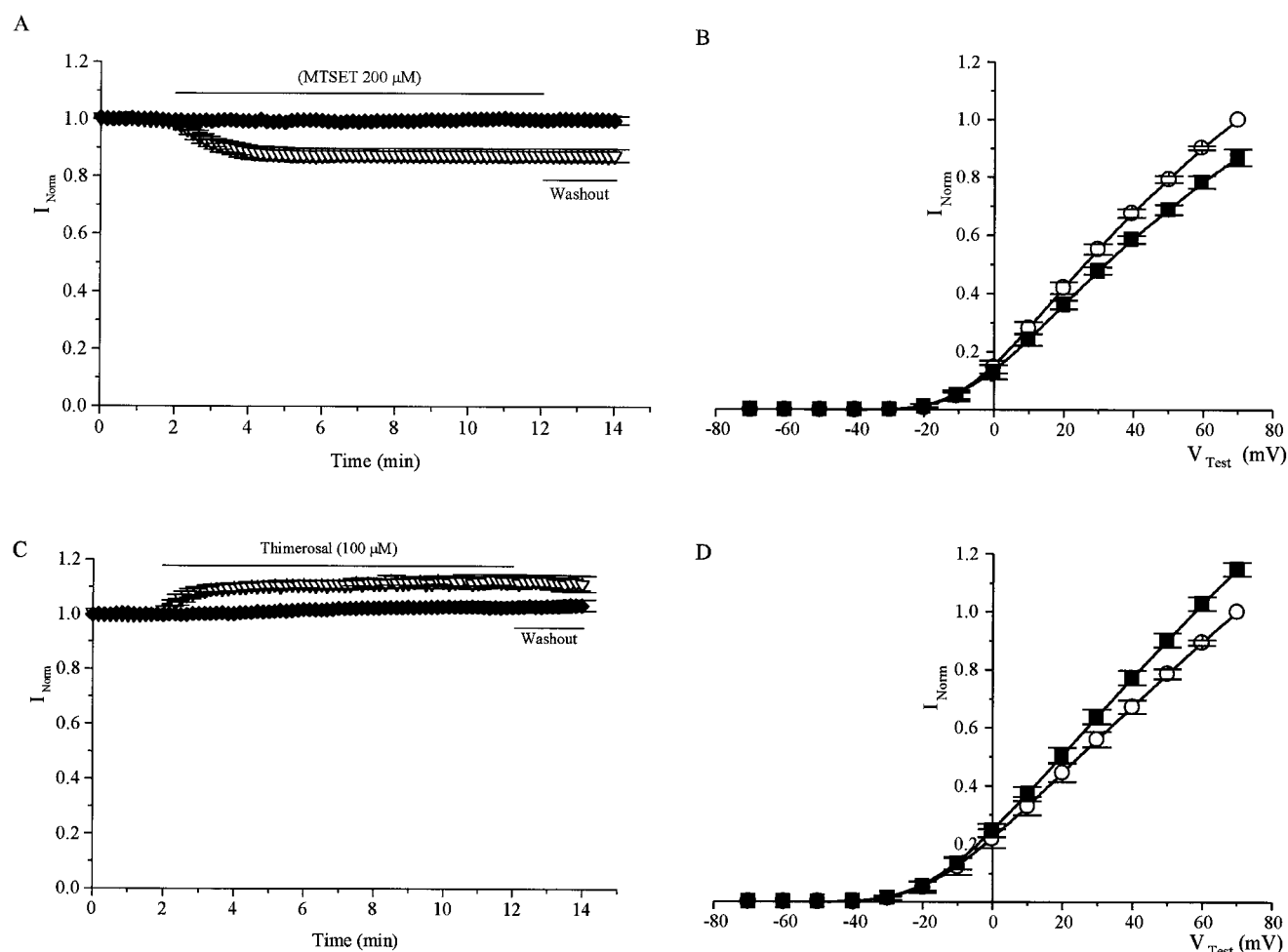


**FIGURE 6** Effects of the cysteine-binding reagents MTSET and thimerosal on mutant S223C current amplitudes. (A) Oocytes were perfused with MTSET (200  $\mu$ M) over the time indicated by the solid bar, and cells were repetitively depolarized by stepping from a holding potential of  $-80$  mV to  $+40$  mV for 500 ms every 10 s. Current amplitudes were normalized to the value recorded over the first 2 min of the experiment. Initial values of current were  $10.3 \pm 0.8$   $\mu$ A,  $n = 4$  (wt) and  $11.5 \pm 0.7$   $\mu$ A,  $n = 3$  (S223C). S223C current amplitude ( $\nabla$ ) was significantly reduced by MTSET ( $p < 0.05$ ) for  $t > 2$  min as compared to wild type and to initial current values. MTSET had no significant effect on the current amplitude for the wild-type channel ( $\blacklozenge$ ). (B) Current-voltage relationship curves before ( $\circ$ ) and after ( $\blacksquare$ ) the application of MTSET (200  $\mu$ M) from the same experiments as in A. Currents were normalized to the value in the absence of MTSET at a test potential of  $+70$  mV ( $I_{\text{Norm}}$ ) (amplitude  $21.9 \pm 3.5$   $\mu$ A,  $n = 3$ ). (C) Oocytes were perfused with thimerosal (100  $\mu$ M) over the time indicated by the solid bar, and cells were repetitively depolarized by stepping from a holding potential of  $-80$  mV to  $+40$  mV for 500 ms every 10 s. Current amplitudes were normalized to the value recorded over the first 2 min of the experiment. Initial values of current were  $6.5 \pm 1.1$   $\mu$ A,  $n = 5$  (wt) and  $14.9 \pm 1.6$   $\mu$ A,  $n = 6$  (S223C). S223C current amplitude ( $\nabla$ ) was significantly increased by thimerosal ( $p < 0.05$ ) for  $t > 2$  min as compared to wild type and to initial current values. MTSET had no significant effect on the current amplitude for the wild-type channel ( $\blacklozenge$ ). (D) Current-voltage relationship curves before ( $\circ$ ) and after ( $\blacksquare$ ) the application of thimerosal (100  $\mu$ M) from the same experiments as above. Currents were normalized to the value in the absence of thimerosal at a test potential of  $+70$  mV ( $I_{\text{Norm}}$ ) (current value  $21.6 \pm 2.8$   $\mu$ A,  $n = 6$ ).

inhibition of the S223C mutant channel might suggest that only a small local conformational change at this residue occurs when the membrane potential is changed; in any case, binding of PCMBs does not seem to have induced major structural changes causing a block of channel function. Absence of use-dependent block suggests that PCMBs binding to the S2 region does not cause open channel block, consonant with the location of S2 away from the pore.

It is interesting that deactivation was speeded up rather than slowed by PCMBs. Possibly interference with the S2 region by PCMBs paradoxically may allow the S4 region to

move back into its resting position faster after hyperpolarization, thus closing the channel faster. This may be relevant to the suggestion that S2 gating charge movement occurs before S4 movement (Seoh et al., 1996; Cha and Bezanilla, 1997) for channel opening and presumably vice versa for channel closing during deactivation.

Our previous work using PCMBs has shown that several contiguous amino acids in the S4 region together become accessible upon depolarization, consistent with a model (among others) of contiguous movement of several amino acids out of the membrane (Yusaf et al., 1996). This con-



trasts with the above results, where effects of PCMBs were seen locally on residue S223 but not on the nearby extracellular residues D225 and N226, which also might be expected to move inward toward the S2 region. Previous work using fluorescent labeling of extracellular S2 cysteine mutants for the *Shaker* channel (Cha and Bezanilla, 1997) has also indicated local but not global movement of the S2 residues; significant changes in fluorescence with membrane potential were found for two residues but not for two other residues nearby. Cha and Bezanilla (1997) found, as we have, that the main effect of cysteine probes was observed at intermediate potentials. Detailed comparison between equivalent residues in *Shaker* and hKv2.1 suggests that *Shaker* T276 corresponds to hKv2.1 N226, and yet there was a voltage-dependent change in fluorescence for T276 in the study of Cha and Bezanilla but no effect for PCMBs in our study for N226. Furthermore, *Shaker* P273 showed no fluorescence changes with potential, while the corresponding residue S223 in hKv2.1 showed voltage-dependent effects. There are several possible explanations for the differences. First, the fluorescent labels sense localized changes in positions of nearby residues, whereas the studies using PCMBs performed here determine accessibility. Clearly the movement of surrounding residues could be such that surrounding residues might move, so affecting fluorescence but without affecting accessibility of PCMBs, and vice versa. Second, the nature of the cysteine-binding probe can affect results; for instance, fluorescent probes with differing charge can produce differing effects at the same residue (Cha and Bezanilla, 1997). Third, differences between different channel clones may be more apparent than real because alignments are uncertain for the nonconserved loop regions; indeed the S1/S2 linker is 12 residues shorter for hKv2.1 than for *Shaker*.

In summary, our results suggest that some of the residues located extracellularly to the S2 region play some role in channel gating. In particular, residue S223 is accessible to PCMBs at normal resting potentials and therefore must be exposed to the extracellular phase. Nearby residues were not available to PCMBs. Upon depolarization, residue 223 becomes less accessible, probably as a result of a local inward movement rather than a simple movement en bloc of the negatively charged S2 region into the membrane.

We thank the Wellcome Trust for support and Prof. O. Pongs for the hKv2.1 clone and mutants A230C and N226C.

## REFERENCES

- Aggarwal, S. K., and R. MacKinnon. 1996. Contribution of the S4 segment to gating charge in the *Shaker* K<sup>+</sup> channel. *Neuron*. 16:1169–1177.
- Albrecht, B., C. Lorra, M. Stocker, and O. Pongs. 1993. Cloning and characterization of a human delayed rectifier potassium channel gene. *Receptors Channels*. 1:99–110.
- Armstrong, C. M. and B. Hille. 1998. Voltage-gated ion channels and electrical excitability. *Neuron*. 20:371–380.
- Baker, O. S., H. P. Larsson, L. M. Mannuzzu, and E. Y. Isacoff. 1998. Three transmembrane conformations and sequence-dependent displacement of the S4 domain in *Shaker* K<sup>+</sup> channel gating. *Neuron*. 20:1283–1294.
- Cha, A., and F. Bezanilla. 1997. Characterizing voltage-dependent conformational changes in the *Shaker* K<sup>+</sup> channel with fluorescence. *Neuron*. 19:1127–1140.
- Choi, K. L., G. Mossman, J. Aube, and G. Yellen. 1993. The internal quaternary ammonium receptor site of *Shaker* potassium channels. *Neuron*. 10:533–541.
- Doyle, A. D., J. M. Cabral, R. A. Pfuetschner, A. Kuo, J. M. Gulbis, S. L. Cohen, B. T. Chait, and R. MacKinnon. 1998. The structure of the potassium channel: molecular basis of K<sup>+</sup> conduction and selectivity. *Science*. 280:69–77.
- Dumont, J. N. 1972. Oogenesis in *Xenopus laevis*. *J. Morphol.* 136:153–180.
- Durell, S. R., and H. R. Guy. 1992. Atomic scale structure and functional models of voltage-gated potassium channels. *Biophys. J.* 62:238–247.
- Hartmann, H. A., G. E. Kirsch, J. A. Drewe, M. Tagliatella, R. H. Joho, and A. M. Brown. 1991. Exchange of conduction pathways between two related K<sup>+</sup> channels. *Science*. 251:942–944.
- Holmgren, M., P. L. Smith, and G. Yellen. 1997. Trapping of organic blockers by closing of voltage-dependent K<sup>+</sup> channels. *J. Gen. Physiol.* 109:527–535.
- Innis, M. A., D. H. Gelfand, J. J. Sninsky, and T. J. White. 1990. PCR protocols. A Guide to Methods and Applications. Academic Press, New York. 177–183.
- Kirsch, G. E., C.-C. Shieh, J. A. Drewe, D. F. Vener, and A. M. Brown. 1993. Segmental exchanges define 4-aminopyridine binding and the inner mouth of K<sup>+</sup> pores. *Neuron*. 11:503–512.
- Larsson, H. P., O. S. Baker, D. S. Dhillon, and E. Y. Isacoff. 1996. Transmembrane movement of the *Shaker* K<sup>+</sup> channel S4. *Neuron*. 16:387–397.
- Liman, E. R., P. Hess, F. Weaver, and G. Koren. 1991. Voltage-sensing residues in the S4 region of a mammalian K<sup>+</sup> channel. *Nature*. 353:752–756.
- Logothetis, D. E., S. Movahedi, C. Slater, K. Lindpaintner, and B. Nadal-Ginard. 1992. Incremental reductions of positive charge within the S4 region of a voltage-gated K<sup>+</sup> channel result in corresponding decreases in gating charge. *Neuron*. 8:531–540.
- Lopez, G. A., Y. N. Yan, and L. Y. Jan. 1994. Evidence that the S6 segment of the *Shaker* voltage-gated K<sup>+</sup> channel comprises part of the pore. *Nature*. 367:179–182.
- MacKinnon, R., and G. Yellen. 1990. Mutations affecting TEA blockade and ion permeation in voltage-activated K<sup>+</sup> channels. *Science*. 250:276–279.
- Mannuzzu, L. M., M. M. Moronne, and E. Y. Isacoff. 1996. Direct physical measure of conformational rearrangement underlying potassium channel gating. *Science*. 271:213–216.
- Mathur, R., J. Zheng, Y. Yan, and F. J. Sigworth. 1997. Role of the S3–S4 linker in *Shaker* potassium channel activation. *J. Gen. Physiol.* 109:191–199.
- Papazian, D. M., X. M. Shao, S.-A. Seoh, A. F. Mock, Y. Huang, and D. H. Wainstock. 1995. Electrostatic interactions of S4 voltage sensor in the *Shaker* K<sup>+</sup> channel. *Neuron*. 14:1293–1301.
- Papazian, D. M., L. C. Timpe, Y. N. Jan, and L. N. Jan. 1991. Alteration of voltage-dependence of *Shaker* potassium channel by mutations in the S4 sequence. *Nature*. 349:305–310.
- Perozo, E., R. MacKinnon, F. Bezanilla, and E. Stefani. 1993. Gating currents from a nonconducting mutant reveal open-closed conformations in *Shaker* K<sup>+</sup> channels. *Neuron*. 11:353–358.
- Planells-Cases, R., A. V. Ferrer-Montiel, C. D. Patten, and M. Montal. 1995. Mutation of conserved negatively charged residues in the S2 and S3 transmembrane segments of a mammalian K<sup>+</sup> channel selectively modulates channel gating. *Proc. Natl. Acad. Sci. USA*. 92:9422–9426.
- Pongs, O. 1992. Structural basis of voltage-gated K<sup>+</sup> channel pharmacology. *Trends Pharmacol. Sci.* 13:359–365.

- Sambrook, J., E. F. Fritsch, and T. Maniatis. 1989. *Molecular Cloning—A Laboratory Manual*. Cold Spring Harbor Laboratory, Cold Spring Harbor, NY.
- Seoh, S.-A., D. Sigg, D. M. Papazian, and F. Bezanilla. 1996. Voltage-sensing residues in the S2 and S4 segments of the *Shaker* K<sup>+</sup> channel. *Neuron*. 16:1159–1167.
- Shao, X., and D. M. Papazian. 1993. S4 mutations alter the single channel gating kinetics of *Shaker* K<sup>+</sup> channels. *Neuron*. 11:343–352.
- Tiwari-Woodruff, S. K., C. T. Schulteis, A. F. Mock, and D. M. Papazian. 1997. Electrostatic interactions between transmembrane segments mediate folding of *Shaker* K<sup>+</sup> channel subunits. *Biophys. J.* 72:1489–1500.
- Wilson, G. G., C. A. O'Neill, A. Sivaprasadarao, J. B. C. Findlay, and D. Wray. 1994. Modulation by protein kinase A of a cloned rat brain potassium channel expressed in *Xenopus* oocytes. *Pflügers Arch.* 428:186–193.
- Yao, J.-A., M. Jiang, and G.-N. Tseng. 1997. Mechanism of enhancement of slow delayed rectifier current by extracellular sulphhydryl modification. *Am. J. Physiol.* 273:H208–H219.
- Yellen, G., M. E. Jurman, T. Abramson, and R. MacKinnon. 1991. Mutations affecting internal TEA blockade identify the probable pore-forming region of a K<sup>+</sup> channel. *Science*. 251:939–942.
- Yool, A. J., and T. L. Schwartz. 1991. Alteration of ionic selectivity of a K<sup>+</sup> channel by mutation of the H5 region. *Nature*. 349:700–704.
- Yusaf, S. P., D. Wray, and A. Sivaprasadarao. 1996. Measurement of the movement of the S4 segment during the activation of a voltage-gated potassium channel. *Pflügers Arch.* 433:91–97.